Intercalation of Well-Dispersed Gold Nanoparticles into Layered Oxide Nanosheets through Intercalation of a Polyamine

Hideo Hata,[†] Shoichi Kubo,[†,‡] Yoji Kobayashi,[†] and Thomas E. Mallouk*,[†]

Department of Chemistry, The Pennsylvania State University, University Park, Pennsylvania 16802 and Chemical Resources Laboratory, Tokyo Institute of Technology, R1-11, 4259 Nagatsuta, Midori-ku, Yokohama 226-8503, Japan

Received November 18, 2006; E-mail: tom@chem.psu.edu

Gold nanoparticles have attracted widespread interest in both materials chemistry and biomedical science because of their special electronic, magnetic, catalytic, and optical properties[1,2] For these applications, it is important to be able to control the size, shape, and dispersion of the nanoparticles on a chemically diverse range of supports. Oxides are among the most interesting kinds of support materials for nanogold, particularly for plasmonic and catalytic applications.[3,4] However, in most of these studies, the nanoparticles are synthesized in situ, and it is difficult to control their size distribution and dispersion on the oxide support.

The layer-by-layer (LBL) assembly of oppositely charged polyelectrolytes and nanoparticles has been widely studied as a route to functional composite materials.[5,6] Structural control in the LBL method derives from the fact that the surface charge inverts in each sequential adsorption step. By adapting this principle to intercalation compounds, we recently showed that one could overcompensate the charge of anionic polysilicate nanosheets by intercalating coiled polycationic chains. This makes the layered solid an anion exchanger, which can intercalate large molecular anions into the cationic interlayer galleries.[7] Because gold and many other kinds of nanoparticles are negatively charged at neutral and alkaline pH, we sought to investigate their intercalation into these cationic hosts.

We report here a general method for intercalating gold nanoparticles (NPs) into the galleries of layered materials. This method allows us to disperse gold NPs within the interlayers of exfoliated fluoromica (Na-TSM) as well as a Dion–Jacobson phase layered perovskite ($HCa_2Nb_3O_{10}$)[8] with little aggregation. With amine polymer-intercalated hosts, the driving force for the reaction is covalent bonding between NPs and the free amine groups of the polymer. With quaternary ammonium polymer modified hosts, intercalation occurs through anion exchange. In both cases, a polymer loading in excess of that needed to compensate the layer charge is required for NP intercalation.

Colloidal Au NPs with diameter of 1–3 nm (Au(S)) or 2–6 nm (Au(L)) were prepared by the method of Pham et al.[9] $HCa_2Nb_3O_{10}$ was made by ion-exchange of $KCa_2Nb_3O_{10}$ in aqueous HNO_3.[10] Poly(allylamine), PAA, was intercalated at pH 12.0–12.5 to minimize protonation of the primary amine groups of the polymer. In the preparation of Au/PAA/Na-TSM (*n*), where *n* denotes the adsorbed amount (in millimoles) of Au per gram of host solid, a PAA/Na-TSM aqueous suspension was added to the appropriate amount of Au NP suspension and stirred at pH 12.0–12.5. After centrifugation, the resulting product was washed thoroughly with water, followed by drying at 333 K. In cases where the reaction did not go to completion, the amount of Au absorbed was calculated by comparing the absorption spectrum of a 0.0625 wt % suspension with that of an intercalation compound of known composition. For
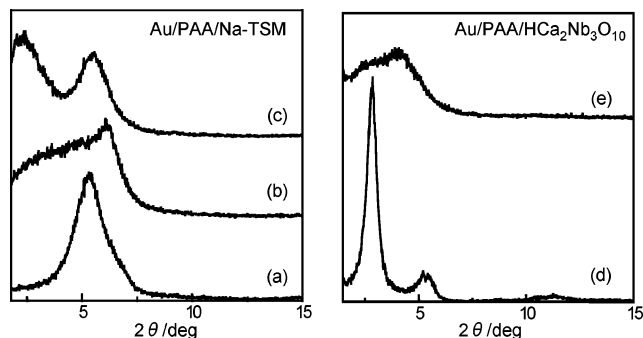
Figure 1. XRD patterns of PAA/Na-TSM (a), Au(S)/PAA/Na-TSM (0.79) (b), Au(L)/PAA/Na-TSM (0.79) (c), PAA/$HCa_2Nb_3O_{10}$ (d), and Au(S)/PAA/$HCa_2Nb_3O_{10}$ (<0.90) (e). The patterns were recorded on Philips X'Pert MPD diffractometer (monochromatized Cu Kα1).

Au/PAA/$HCa_2Nb_3O_{10}$, the same procedure was followed except that the solid was exfoliated using tetra(*n*-butyl)ammonium hydroxide before intercalation of PAA.

Figure 1 shows typical XRD patterns of PAA/Na-TSM and PAA/$HCa_2Nb_3O_{10}$ before and after Au intercalation. The basal plane spacings of Na-TSM and $HCa_2Nb_3O_{10}$ prior to intercalation were 9.6 and 14.7 Å, respectively. After intercalation of PAA into Na-TSM or $HCa_2Nb_3O_{10}$ (Figure 1a and 1d), the spacings increased to 16.5 and 30.9 Å, respectively, indicating intercalation of coiled PAA chains. The coiled chains contain ionizable amine groups in excess of that needed to compensate the anionic charges of the sheets.[7] The larger change in spacing in the case of $HCa_2Nb_3O_{10}$ reflects the higher charge density of the sheets relative to Na-TSM. After intercalation of Au(S) into PAA/Na-TSM (Figure 1b), a broad shoulder was observed at d = 20–35 Å. For Au(L)/PAA/Na-TSM (Figure 1c), a more prominent diffraction peak was observed at a *d*-spacing of 35–45 Å, indicating that the larger Au(L) NPs were also accommodated by the interlayer galleries. The XRD patterns of Au/PAA/Na-TSM both show an additional phase with shorter gallery height (15–16 Å) than PAA/Na-TSM. In this phase the PAA chains must lie flat, and they do not accommodate intercalated NPs. Similar behavior was observed in the intercalation of large molecular anions into polycation/Na-TSM composites.[7] The same pattern of reactivity was found with $HCa_2Nb_3O_{10}$, PAA, and Au NPs. A broad shoulder was observed at d = 32–38 Å, indicating intercalation of Au NPs. As in the case of the Na-TSM host, a broad peak was observed on the high-angle side of the original diffraction peak, indicating the formation of a second phase with a single flat layer of intercalated polymer.

TEM images of Au(S) and (L)/PAA/Na-TSM and Au(S)/PAA/$HCa_2Nb_3O_{10}$ (Figure 2a, b, and c), show that the Au NPs, regardless of particle size and host material, are well-dispersed within the interlayer. From TEM image analysis,[11] the average NP diameters for Au(S)/PAA/Na-TSM (0.79 and 0.20) were 1.7 ± 0.6 and 1.3

---

† The Pennsylvania State University.
‡ Tokyo Institute of Technology.
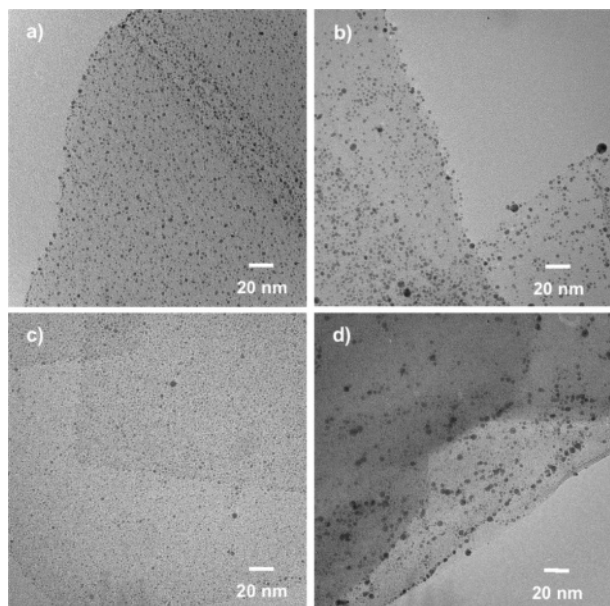
Figure 2. Typical TEM images of Au(S)/PAA/Na-TSM (1.27) (a), Au(L)/PAA/Na-TSM (0.79) (b), Au(S)/PAA/HCa$_2$Nb$_3$O$_{10}$ (<0.90) (c), and Au(S)/PDDA/Na-TSM (0.40). The images were obtained by Philips 420T microscope at an accelerating voltage of 120 kV.

± 0.4 nm, indicating that little aggregation or coalescence of particles occurs even at high loading. Image analysis showed that NP nearest neighbor distances in Au(S)/PAA/Na-TSM (0.79 and 0.20) were 2.6 ± 0.8 and 5.5 ± 2.6 nm, respectively. At high loading of Au(L) (>0.79) (Supporting Information, Figure S1c), we could observe some larger aggregates on the outer surface of the composites, which implies that movement into the galleries is restrained with increasing NP size.

It is well-known that primary amines can make weak covalent bonds at the surface of Au NPs.[12] In the FTIR spectra (see Supporting Information) of PAA/Na-TSM, peaks due to the free primary amine groups were observed at 3377 cm^{-1}(v_{as} N−H), 3277 cm^{-1}(v_s N−H), and 1568 cm^{-1} (δ_s N−H). An additional peak at 1633 cm^{-1} was attributed to the scissoring vibration of NH groups interacting strongly with the sheets. With increasing Au loading, we observe decreases in the peak intensity ratios of v_{as} to v_s and δ_s (1568 cm^{-1}) to δ_s (1633 cm^{-1}). These spectral features are consistent with N−Au bonding as the driving force for intercalation of NPs. When PAA was replaced to a quaternary polycation, poly-(diallyldimethylammonium) (PDDA), Au NPs were also intercalated, but with significant aggregation within the galleries (average particle size: 4.2 ± 1.2 nm, Figure 2d). In the PDDA case, NP intercalation is driven by electrostatic interaction between the negatively charged Au surface and cationic ammonium groups, and this weaker interaction results in aggregation. As a control experiment, sodium dodecyl sulfate (SDS) was reacted with PAA or PDDA/Na-TSM at pH 12.0−12.5. SDS could be intercalated only into PDDA/Na-TSM, (see Supporting Information), indicating that the electrostatic driving force is not sufficient to drive anion intercalation in the PAA case. Taken together, the data support the idea that Au NP intercalation can be driven either by N−Au bonding or by electrostatic interactions, and that the former mechanism dominates in the case of PAA intercalated Na-TSM and HCa$_2$Nb$_3$O$_{10}$.

UV−visible absorption spectra of the composite particles (see Supporting Information) are consistent with the TEM images. For Au(L)/PAA/Na-TSM (0.39), in which very little aggregation is apparent by TEM, the plasmon resonance maximum of Au NPs peaks at 525 nm, a slight red-shift relative to the original solution (510 nm). Similar red-shifts occur for Au(S)/PAA/Na-TSM and /HCa$_2$Nb$_3$O$_{10}$. It is well-known that the plasmon resonance absorption maximum is sensitive to the dielectric properties of the medium, and we attribute the small red-shift to this effect.

For some applications, including heterogeneous catalysis, it would be desirable to remove PAA from the interlayer to convert the layered composites into Au-pillared porous materials. Our preliminary experiments showed that calcination of the samples at 1073 K to remove PAA led to aggregation of the Au NPs. We are currently experimenting with lower temperature methods for eliminating PAA without causing NPs aggregation.

In conclusion, we have demonstrated the intercalation of Au NPs into the 2D galleries of two different layered oxides through pre-intercalation of polyamine chains. The Au NPs were well dispersed within the interlayer galleries, on the basis of TEM observations. Covalent bonding between primary amine groups of the PAA chains and the Au NP surface appears to drive the intercalation reaction. This convenient route to well dispersed NPs intercalated into lamellar oxides may have utility in catalytic, optical, and possibly biomedical applications of nanogold.

Supporting Information Available: Materials and detailed experimental procedures, TEM images of Au NPs and Au(L)/PAA/Na-TSM (>0.79), FTIR spectra of PAA/Na-TSM and Au(S)/PAA/Na-TSM, XRD patterns of Au(S)/PDDA/Na-TSM, SDS/PAA/Na-TSM, and SDS/PDDA/Na-TSM, and UV−vis absorption spectra of an as-prepared Au(L) suspension and 0.625 wt % Au(L)/PAA/Na-TSM (0.39). This material is available free of charge via the Internet at http://pubs.acs.org.

References

(1) Alivisatos, A. P. *Nat. Biotechnol.* **2004**, *22*, 47.
(2) (a) Haruta, M. *Catal. Today* **1997**, *36*, 153. (b) Valden, M.; Lai, X.; Goodman, D. W. *Science* **1998**, *281*, 1647. (c) Narayanan, R.; El-Sayed, M. A. *J. Phys. Chem. B* **2005**, *109*, 12663.
(3) (a) Yan, Z.; Chinta, S.; Mohamed, A. A.; Fackler, J. P.; Goodman, D. W. *J. Am. Chem. Soc.* **2005**, *127*, 1604. (b) Shi, F.; Zhang, Q.; Ma, Y.; He, Y.; Deng, Y. *J. Am. Chem. Soc.* **2005**, *127*, 4182. (c) Zheng, N.; Stucky, G. D. *J. Am. Chem. Soc.* **2006**, *128*, 14278.
(4) (a) Wang, H.; Brandl, D. W.; Nordlander, P.; Halas, N. J. *Acc. Chem. Rec.* **2007**, *40*, 53. (b) Schuetz, P.; Caruso, F. *Chem. Mater.* **2004**, *16*, 3066. (c) Zhu, J.; Kónya, Z.; Puntes, V. F.; Kiricsi, I.; Miao, C. X.; Ager, J. W.; Alivisatos, A. P.; Somorjai, G. A. *Langmuir* **2003**, *19*, 4396. (d) Gupta, G.; Shah, P. S.; Zhang, X.; Saunders, A. E.; Korgel, B. A.; Johnston, K. P. *Chem. Mater.* **2005**, *17*, 6728. (e) Ma, R.; Sasaki, T.; Bando, Y. *J. Am. Chem. Soc.* **2004**, *126*, 10382. (f) Ide, Y; Fukuoka, A.; Ogawa, M. Chem. Mater., published online Feb 2, 2007, http://dx.doi.org/10.1021/cm062117d.
(5) Dacher, G.; Schlenoff, J. B. *Multilayer Thin Films*; Wiley-VCH Verlag GmbH & Co. KGaA: Weinheim, Germany, 2003.
(6) Caruso, F. *Adv. Mater.* **2001**, *13*, 11.
(7) Hata, H.; Kobayashi, Y.; Mallouk, T. E. *Chem. Mater.* **2007**, *19*, 79.
(8) Individual sheets of exfoliated niobates have been decorated with Au nanoparticles using (3-aminopropyl)trimethoxysilyl linkers: Kim, Y. J.; Osterloh, F. E. *J. Am. Chem. Soc.* **2006**, *128*, 3868.
(9) Pham, T.; Jackson, J. B.; Halas, N.; Lee, T. R. *Langmuir* **2002**, *18*, 4915.
(10) Fang, M.; Kim, C. H.; Saupe, G. B.; Kim, H.-N.; Waraksa, C. C.; Miwa, T.; Fujishima, A.; Mallouk, T. E. *Chem. Mater.* **1999**, *11*, 1526.
(11) Image analysis was performed using the public domain software ImageJ (developed at the U.S. National Institutes of Health and available on the Internet at http://rsb.info.nih.gov/nih-image/).
(12) (a) Leff, D. V.; Brandt, L.; Heath, J. R. *Langmuir* **1996**, *12*, 4723. (b) Kumar, A.; Mandal, S.; Selvakannan, P. R.; Pasricha, R; Mandale, A. B.; Sastry, M. *Langmuir* **2003**, *19*, 6277.

JA068272A